PROCEEDINGS OF SCIENCE

Indication of population effect in UHECR sources

Quentin Luce,[a,*] **Jonathan Biteau,**[a,b] **Olivier Deligny**[a] **and Antonio Condorelli**[c]

[a] *Université Paris-Saclay, CNRS/IN2P3, IJCLab, Orsay (France)*

[b] *Institut Universitaire de France (France)*

[c] *Université Paris Cité, CNRS, Astroparticule et Cosmologie, F-75013 Paris, France*

E-mail: quentin.luce@ijclab.in2p3.fr, jonathan.biteau@ijclab.in2p3.fr

The Ultra-High Energy Cosmic Rays (UHECRs) are nuclei carrying the highest energy ever measured on Earth. The first particle with an energy above 10^{20} eV was already observed in the 1960s. But, after 60 years of observations, the sources of UHECRs remains uncertain. To tackle this unresolved question, the Pierre Auger Observatory, the largest observatory ever built, has recorded the detection of UHECRs over the past 20 years and reconstructed with an unprecedented precision their energy spectrum, mass composition and arrival directions, together with its smaller counterpart in the Northern hemisphere, the Telescope Array.

Studies assuming a distribution of identical sources, which aim at reproducing the energy spectrum and the mass composition data above $10^{17.8}$ eV, have led to the paradigma of acceleration processes of UHECRs in extragalactic accelerators that depend on the magnetic rigidity of the particles. Coupled with the interaction processes in the intergalactic medium, such models result in a very hard spectral index at escape from the source. Such models have recently been improved considering the in-source interactions and the resulting escape of neutrons, which yields a softer spectral index for the proton component.

In this contribution, we evaluate approaches that go beyond the hypothesis of identical sources and account in an effective manner for the variety of the acceleration and escape mechanisms that a population of sources may encompass. We discuss the implications of the fact that, while the range of the maximum rigidity is limited, a large diversity of spectral indices appears to be preferred by the modeling of the data.

39th International Cosmic Ray Conference (ICRC2025)
15–24 July 2025
Geneva, Switzerland

*Speaker

PoS(ICRC2025)322

1. Introduction

Ultra-high energy cosmic rays (UHECRs), discovered in the 20th century, are still the subject of thorough study to determine the sources and the mechanisms that accelerate particles to energies as high as 10^{20} eV, the highest ever observed. The Pierre Auger Observatory [1], a dedicated project located in the Argentinian Pampa, has collected more than two decades of data to address this century-old question. The origins of the UHECRs remain elusive but we are closing in on the answer. Indeed, the Pierre Auger Collaboration reported a study of anisotropies at large scales in the arrival directions of the cosmic rays with energies above $\simeq 8 \times 10^{18}$ eV which proved the existence of a dipole with a significance larger than 5σ [2]. The intensity and the pointing direction of the reconstructed dipole are consistent with an extragalactic origin of the highest-energy cosmic rays.

This interpretation aligns with the several features exhibited by the shape of the energy spectrum of UHECRs. The hardening of the spectrum observed at $\simeq 5 \times 10^{18}$ eV, called the ankle, and the significant suppression of the flux observed on Earth for energies above 5×10^{19} eV have been reported by early experiments observing UHECRs such as Haverah Park, AGASA, and HiRes. These findings have been validated with an unprecedented precision by the Pierre Auger Observatory [3]. While the suppression is interpreted as the result of the propagation of UHECRs from the sources to Earth, the situation is unclear below the energy of the ankle. One possible interpretation of the observed hardening is a transition between two origins of the cosmic rays: the exhaustion of a Galactic production of UHECRs below the ankle and an extragalactic production above it.

More recent studies have modeled the Pierre Auger Observatory's composition data and the energy spectrum by assuming a rigidity-dependent mechanism for accelerating UHECRs up to the maximum rigidity $R_{\rm max}$ of an exponential cutoff, commonly denoted as Peters' cycle. The evolution with energy of the mean and variance of the distribution of the maximum shower development $X_{\rm max}$ [4], used as an estimator of the mass of the cosmic rays, supports a succession of mono-elemental components above the ankle energy. A possible interpretation of the composition data and energy spectrum of UHECRs for energies above $10^{17.8}$ eV is presented in [5], where an astrophysical model with two extragalactic source populations is considered to explain the hardening at the ankle. In this benchmark scenario, a mixed composition with a hard spectrum and a low rigidity cutoff is necessary for the high-energy extragalactic component to best reproduce the observations. In contrast, the low-energy extragalactic component requires a soft spectrum and a mixture of protons and intermediate-mass nuclei, the origin of which is unknown. However, constraining such a complex scenario without a precise knowledge of the end of the Galactic component of the cosmic-ray flux is challenging.

Additionally, this scenario does not fully account for the interactions that accelerated nuclei encounter within or near the sources. These interactions lead to a more complex escape spectrum of nuclei than Peters' cycle. Including in-source interactions in the modeling of the escape spectrum of cosmic rays reveals a harder spectrum than expected from standard acceleration mechanisms, as well as the ejection of neutrons that decay into protons en route to Earth [6]. An alternative parametrization has been considered to fit the data of the Pierre Auger Observatory using a model in which protons and nuclei are described by energy spectra with a different spectral index γ_A for nuclei and γ_p for protons. To constrain the spectral index of the proton component, the proton

spectrum is extracted by multiplying the all-particle spectrum and the fraction of protons derived from the composition data. The best-fit model obtained recovers previous results, which require nuclei to be accelerated with a hard spectral index for the all-particle spectrum. Below the ankle, the observed population of protons is better reproduced with a significantly softer spectral index than that of higher-mass nuclei constraining the origins of the protons arriving at Earth [7, 8].

Due to the model's complexity, the benchmark scenario used to describe the data of composition and the energy spectrum of UHECRs assumes identical sources. In this study, we present a method to relax this assumption by incorporating in the scenario a dispersion of the parameters shaping the escape spectrum of UHECRs: the maximum rigidity $R_{\rm max}$ and the spectral indices γ_A and γ_p. Section 2 details the main ingredients necessary for the combined fit of the energy spectrum and the composition data of the Pierre Auger Observatory, using the mathematical framework of the convolution of the spectrum with the distribution of the spectral index and/or the maximum rigidity. The results of the best-fit are reported and discussed in Section 3, along with a comparison to the best-fit results obtained in a previously published study.

2. Modeling of the UHECR spectrum and composition

2.1 Description of non-identical sources

Following the model described in [8], the ejection rate per unit energy of a cosmic ray with atomic and mass numbers (Z, A) that is accelerated at ultra-high energies and escapes a source at a redshift z is expressed as:

$$\dot{q}_{A/p}(R, z) = \frac{p_{A/p}(R)}{ZR} \varepsilon_{A/p} S(z). \tag{1}$$

$\varepsilon_{A/p}$ is the total injected energy per stellar mass expressed in erg $\mathrm{M}_\odot^{-1}$ and $S(z)$ corresponds to the star-formation rate density [9]. The probability density function for the emitted rigidity R is

$$p_{A/p}(R) = \frac{R \left(\frac{R}{R_0}\right)^{-\gamma_{A/p}} f_{\rm supp}(R)}{Z \int_{R_{\rm max}}^{\infty} R \left(\frac{R}{R_0}\right)^{-\gamma_{A/p}} f_{\rm supp}(R) \mathrm{d}R}, \tag{2}$$

with the reference rigidity R_0 fixed to 10^{18} V. The shape of the suppression of the escaped spectra of UHECRs is commonly described as

$$f_{\rm supp}(R) = \begin{cases} 1 & \text{if } R < R_{\rm max}, \\ \exp\left(1 - \frac{R}{R_{\rm max}}\right) & \text{otherwise.} \end{cases}$$

Several papers have already explored the impact of the shape of the end of the escaped spectrum, see e.g. [5, 10]. Although heavy-side functions are not ideal for modeling the end of the flux of escaping cosmic rays, hyperbolic secant, exponential, and broken-exponential functions do not significantly impact the best-fit parameters obtained. In Eqs. (1) and (2), the indices A are for the nuclei and the index p for the protons. To simplify subsequent formulas, these two indices are omitted. In the absence of explicit notation, the formulas are valid for both nuclei and protons.

The normalization term in Eq. (2) is parameterized as:

$$N(R,\gamma,R_{\max}) = \int_{R_{\min}}^{\infty} R\left(\frac{R}{R_0}\right)^{-\gamma} f_{\rm supp}(R)\mathrm{d}R = \begin{cases} R_0^2\left(\ln\left(\frac{R_{\max}}{R_{\min}}\right) + \mathrm{e}\Gamma(0,1)\right) & \text{if } \gamma = 2, \\ R_0^{\gamma}\left[R_{\max}^{2-\gamma}\left(\frac{1}{2-\gamma} + \mathrm{e}\Gamma(2-\gamma,1)\right) - \frac{R_{\min}^{2-\gamma}}{2-\gamma}\right] & \text{otherwise.} \end{cases} \tag{3}$$

where $\Gamma(x,y)$ is the incomplete gamma function. The minimum rigidity value considered in this study $R_{\min}$ is arbitrarily fixed to $10^{17.5}$ V.

At this point, it is assumed that each source of UHECRs exhibits an identical ejection spectrum. In other words, the escape spectrum of each source is described by the same indices γ_A, γ_p, as well as the same maximum rigidity $R_{\max}$. To test for a non-identical population of sources, the spectral indices and/or the maximum rigidity are varied [10]. The simplest hypothesis is a Gaussian distribution for each spectral parameter, with dispersions of σ_γ for the spectral indices and $\sigma_{R_{\max}}$ for logarithm of the maximum rigidity. The in-source interactions occurring in a second stage, we do not assume a need for a different dispersion of the proton spectral index.

To implement the variations in spectral parameters, we convolve the probability density function of emitted energy (Eq. (2)) with Gaussian distributions in γ and in $\lg R_{\max}$. We call $p_\gamma(R,\gamma,R_{\max})$, the convolution of $p_{A/p}(R)$ with a Gaussian distribution in γ:

$$p_\gamma(R,\gamma,R_{\max}) = p_{A/p}(R) * \mathcal{N}(0,\sigma_\gamma) = \frac{f_{\rm supp}(R)}{\sqrt{2\pi}\sigma_\gamma Z}\int_{-\gamma_b}^{\gamma_b} \frac{R\left(\frac{R}{R_0}\right)^{-\gamma'}\exp\left(-\frac{1}{2}\left(\frac{\gamma-\gamma'}{\sigma_\gamma}\right)^2\right)}{N(R,\gamma',R_{\max})}\mathrm{d}\gamma'. \tag{4}$$

For numerical convenience, the boundaries of the integral are fixed to $\pm\gamma_{\rm b} = \pm 10$. Following the formula for the spectral index, the convolution of $p_{A/p}(R)$ with a Gaussian distribution in $\lg R_{\max}$ is written as

$$\begin{aligned} p_{R_{\max}}(R,\gamma,R_{\max}) &= p_{A/p}(R) * \mathcal{N}(0,\sigma_{R_{\max}}) \\ &= \frac{R\left(\frac{R}{R_0}\right)^{-\gamma}}{\sqrt{2\pi}\sigma_R Z}\int_{\lg R_{\min}}^{\infty}\frac{\mathrm{d}\lg R'_{\max}}{N(R,\gamma,R'_{\max})} f_{\rm supp}(R,R'_{\max})\exp\left(-\frac{1}{2}\left(\frac{\lg R_{\max}-\lg R'_{\max}}{\sigma_{R_{\max}}}\right)^2\right). \end{aligned} \tag{5}$$

Finally, accounting for variations in both γ and $\lg R_{\max}$, the probability density function is expressed as follows:

$$\begin{aligned} p_{\gamma,R}(R,\gamma,R_{\max}) &= p_{A/p}(R) * \mathcal{N}(0,\sigma_\gamma) * \mathcal{N}(0,\sigma_{R_{\max}}) \\ &= \frac{1}{2\pi Z\sigma_\gamma\sigma_{R_{\max}}\sqrt{1-\rho^2}}\int_{-\gamma_b}^{\gamma_b}\int_{\lg R_{\min}}^{\infty}\frac{R\left(\frac{R}{R_0}\right)^{-\gamma'} f_{\rm supp}(R,R'_{\max})}{N(R,\gamma',R'_{\max})}\mathrm{d}\lg R'_{\max}\mathrm{d}\gamma' \\ &\times\exp\left[-\frac{1}{2(1-\rho^2)}\left(\left(\frac{\gamma-\gamma'}{\sigma_\gamma}\right)^2 + \left(\frac{\lg R_{\max}-\lg R'_{\max}}{\sigma_R}\right)^2 - 2\rho\left(\frac{(\gamma-\gamma')(\lg R_{\max}-\lg R'_{\max})}{\sigma_\gamma\sigma_R}\right)\right)\right]. \end{aligned} \tag{6}$$

In Eq. (6), the parameter ρ accounts for the correlation between the spectral index and the maximum rigidity. In a scenario with more in-source interactions, the spectral index γ is expected to be harder, and the maximum rigidity is expected to be reached at smaller energies. To reduce the computational time of the fit procedure, the results of the convolution of Eqs. (6), (4) and (5) are tabulated at discrete values of σ_γ, $\sigma_{R_{\max}}$, γ, $\lg R_{\max}$ and $\lg R$ for values of $\rho = 0, \pm 0.25, \pm 0.75$.

2.2 Propagation and fit

The all-particle spectrum observed on Earth is expressed as

$$J(E) = \frac{c}{4\pi} \sum_{A,A'} \iint \mathrm{d}z\, \mathrm{d}E' \left|\frac{\mathrm{d}t}{\mathrm{d}z}\right| \dot{q}_{A'}(E', z) \frac{\mathrm{d}\eta_{AA'}(E, E', z)}{\mathrm{d}E}, \tag{7}$$

where $E = ZR$. The integration is performed over lookback time using a standard cosmological model encompassed in $|\mathrm{d}t/\mathrm{d}z| = \left(H_0(1+z)\sqrt{(1+z)^3\Omega_\mathrm{m} + \Omega_\Lambda}\right)^{-1}$ with $H_0 = 70\,\mathrm{km\,s^{-1}\,Mpc^{-1}}$, $\Omega_\mathrm{m} = 0.3$ and $\Omega_\Lambda = 0.7$. The term $\eta_{AA'}(E, E', z)$ describes the energy losses and spallation processes and represents the fraction of particles observed at Earth with energy E and mass number A from parent particles emitted by the sources with energy $E' \geq E$ and mass numbers $A' \geq A$. The function $\eta_{AA'}(E, E', z)$ is calculated by simulating the propagation of millions of particles for 5 masses (p, He, CNO, Si, Fe) with the SimProp v2r4 package taking into account pair production, photo-pion production and photodisintegration on the cosmic microwave background and the extragalactic background light. The propagation of cosmic rays through magnetic fields is not considered in this study. The reconstruction of the estimator of the mass of the cosmic ray, X_max is ensured using the hadronic interaction generators Sibyll2.3d and EPOS-LHC.

The fitting procedure involves comparing the simulated energy spectrum obtained using Eq. (7) and the distribution of the mean and variance of X_max associated with the data recorded by the Pierre Auger Observatory [3, 4] above the ankle energy. Below $10^{18.7}$ eV, only the proton contribution to the spectrum is considered. The free parameters are the maximum rigidity R_max, the index of the escaped spectrum for nuclei, the index of the spectrum of protons and the five injected energy per stellar mass, $\varepsilon_{A/p}$. The parameters σ_γ and/or σ_{R_max} are also set free in the procedure.

3. Results and discussion

The best-fit parameters are reported in Table 1 for the benchmark scenario in [8], as well as scenarios including a dispersion of the spectral index (Eq. (4)) and a dispersion of the maximum rigidity (Eq. (5)). Finally, there is a scenario that considers a dispersion of the spectral index and maximum rigidity (Eq. (6)). In every case where a non-identical population of sources is considered, the best-fit parameters are obtained for a value of the correlation parameter $\rho = 0$.

According to Eq. (3), a dependence on the minimum considered rigidity R_min is introduced. We checked that this value does not affect the results as long as it is below the minimum energy of the considered data, $10^{17.8}$ eV. Extending the fit to lower energies would require precise knowledge of the composition in this region, which is not available to date.

In a scenario considering a dispersion in R_max only, the best value of σ_{R_max} is 0.06 ± 0.04, with a p-value of $\simeq$1.9%. Allowing for a large dispersion in the maximum rigidity at which a source can accelerate UHECRs, implies the existence of a population of sources bursting across the sky at the highest energies as seen in Fig. 1. These sources would then appear as bright spots in the studies of the anisotropy of the arrival directions of cosmic rays. However, the absence of such bright spots at the highest energies disfavors such scenario. Requiring a narrow distribution of the maximum rigidity recovers the results reported in [10], in which the authors considered several maximum rigidity distributions.

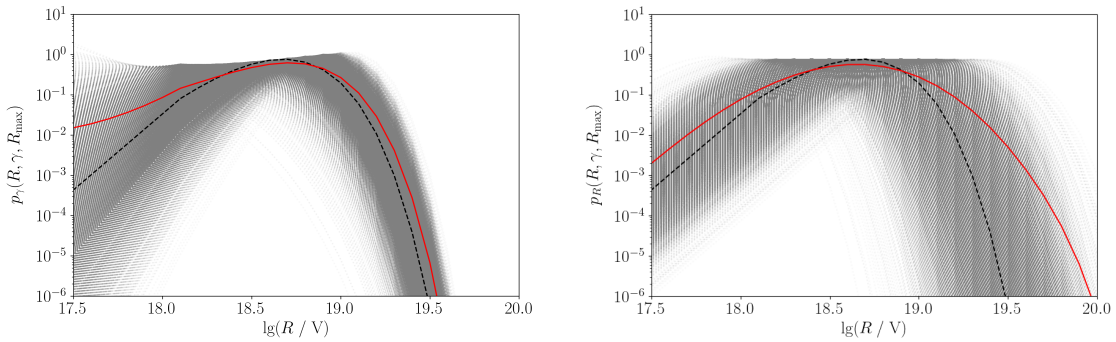

Figure 1: *Left*: Emitted spectrum convolved with a Gaussian distribution in the spectral index of width $\sigma_\gamma = 1.4$ for $\gamma = -1.78$ and $R_{\max} = 10^{18.1}$ V. *Right*: Convolution with a Gaussian distribution in the logarithm of the maximum rigidity of width $\sigma_{R_{\max}} = 0.2$ for $R_{\max} = 10^{18.1}$ V and $\gamma = -1.78$. The black lines represent the *standard* probability density function for the emitted energy following Eq. (2). Each grey line is a realization of Eq. (2) with a value of the spectral index or the maximum rigidity sampled according to the respective Gaussian distribution. The red lines represent the result of the convolution in γ (or in lg $R_{\max}$) following Eq. (4) (or Eq. (5)).

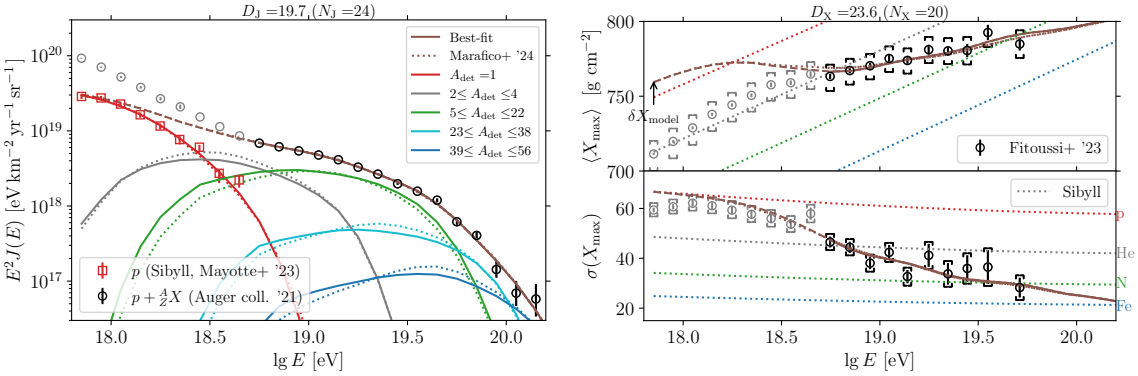

Figure 2: The energy spectrum (*left*) and $X_{\max}$ moments (right) of UHECRs observed on Earth as a function of the energy. This is modeled by the best-fit parameters for a scenario involving the convolution of the probability density function of the emitted energy of an UHECR with Gaussian distributions in the spectral index and in the maximum rigidity.

However, considering sources that eject UHECRs with a distribution of the spectral indices γ_A and γ_p improves the best-fit deviance by 14 points with a distribution of width $\sigma_\gamma = 1.6^{+0.4}_{-0.5}$ (p-value of 16.6%). A p-value of 13.2% is obtained when varying the spectral indices and the maximum rigidity simultaneously with a width $\sigma_\gamma = 1.4^{+0.6}_{-0.3}$. The best-fit results for the latter case (solid lines), along with the results of the benchmark scenario (dashed lines), are shown in Fig. 2. These results suggest a heavier composition at the lowest energies considered with an increased proportion of nitrogen at the expense of helium. At the highest energies, there is a lighter composition, with an increased proportion of nitrogen at the expense of silicon or iron. Similar behaviors are observed when considering EPOS-LHC as the hadronic interaction model.

In Fig. 3, the viable range of the parameters σ_γ and $\sigma_{R_{\max}}$ is assessed by performing a scan of the deviance (related to the best-fit deviance) over the pair of parameters $(\sigma_\gamma, \gamma_A)$ using Eq. (4) and

	benchmark scenario [8]	γ conv.	lg $R_{\rm max}$ conv.	γ+lg $R_{\rm max}$ conv.
$\lg(R_{\rm max}/V)$	18.28±0.04	18.06±0.02	18.24±0.03	18.10±0.01
γ_A	-0.36±0.21	-2.1±0.8	-0.7±0.2	-1.8±0.8
γ_p	2.6±0.7	3.8±0.2	2.7±0.1	3.5±0.4
$\varepsilon_{\rm tot} \times 10^{46}$ erg $M_\odot^{-1}$	4.8±0.2	6.1±0.3	4.9±0.2	5.8±0.4
$f_{\rm H}$ / %	19±4	38±4	22±5	36±7
$f_{\rm He}$ / %	14±3	4±3	14±3	4±2
$f_{\rm CNO}$ / %	48±4	45±4	48±4	46±2
$f_{\rm Si}$ / %	15±3	11±3	13±3	11±3
$f_{\rm Fe}$ / %	4±1	2±1	3±1	3±1
δ_X	1.2±0.2	1.3±0.1	1.1±0.2	1.3±0.2
$D_J + D_X$ (d.o.f.)	22.2+32.1 (36)	20.3+22.7 (35)	21.4+33.1 (35)	19.7+23.6 (34)
σ_γ	-	$1.6^{+0.4}_{-0.5}$	-	$1.4^{+0.6}_{-0.3}$
$\sigma_{R_{\rm max}}$	-	-	0.06±0.04	$\leq$ 0.1 (95% C.L.)

Table 1: Best-fit parameters of the benchmark scenario (reported in [8]), scenarios of a convolution of the probability density function of the emitted energy of an UHECR with a Gaussian distribution in the spectral index, a convolution with a Gaussian distribution in the maximum rigidity and a convolution with Gaussian distributions in both the spectral index and in the maximum rigidity. The results have been produced using Sibyll2.3d as the hadronic interaction model.

over the couples of parameters $(\sigma_{R_{\rm max}}, R_{\rm max})$ and $\sigma_\gamma, \sigma_{R_{\rm max}}$ using Eq. (6).

Looking at Fig. 3-(top-left), it is interesting to note that a strong correlation exists between the spectral index γ_A and the width of the considered Gaussian distribution σ_γ. The greater the dispersion of the spectral index, the harder the ejected spectra of the UHECRs. Thus the fitting procedure for the observed data developed in this study must mitigate the hardening of the mean spectrum of UHECRs, either by fitting values of γ_A close to -1 and values of σ_γ close to 1, or by enlarging the dispersion $\sigma_\gamma \simeq 2$ which hardens each ejected spectrum individually, $\gamma_A \simeq -3$.

As previously noted, our model favors low dispersion of the maximum rigidity. Fig. 3-(top-right) confirms this, showing that the range of values of $\sigma_{R_{\rm max}}$ within the 1σ-contour does not extend beyond 0.05 for values of $\lg R_{\rm max} = 18.1^{+0.02}_{-0.06}$. Combining these behaviors leads to the results presented in Fig. 3-bottom, where the dispersion parameters σ_γ and $\sigma_{R_{\rm max}}$ are bound to [1.1, 2] and [0, 0.06] respectively. Although allowing variations of $\lg R_{\rm max}$ across the source population results in a slight decrease of its average value, the best-fit spectral index and maximum rigidity appear to be largely independent.

Finally, the scenario developed in this study is more favorable to positive a correlation between the spectral index and the maximum rigidity than a negative one. Testing the correlation coefficient at a value of $\rho = +0.75$ leads to an increase in interactions in the near environment of the sources, reflected by an increase of the spectral index for protons only and a slightly harder spectral index for heavier injected elements. Once again, the mean maximum rigidity remains stable but with such a positive correlation, the allowed dispersion of $\lg R_{\rm max}$ increases to approximately 0.15 within the 95% confidence level.

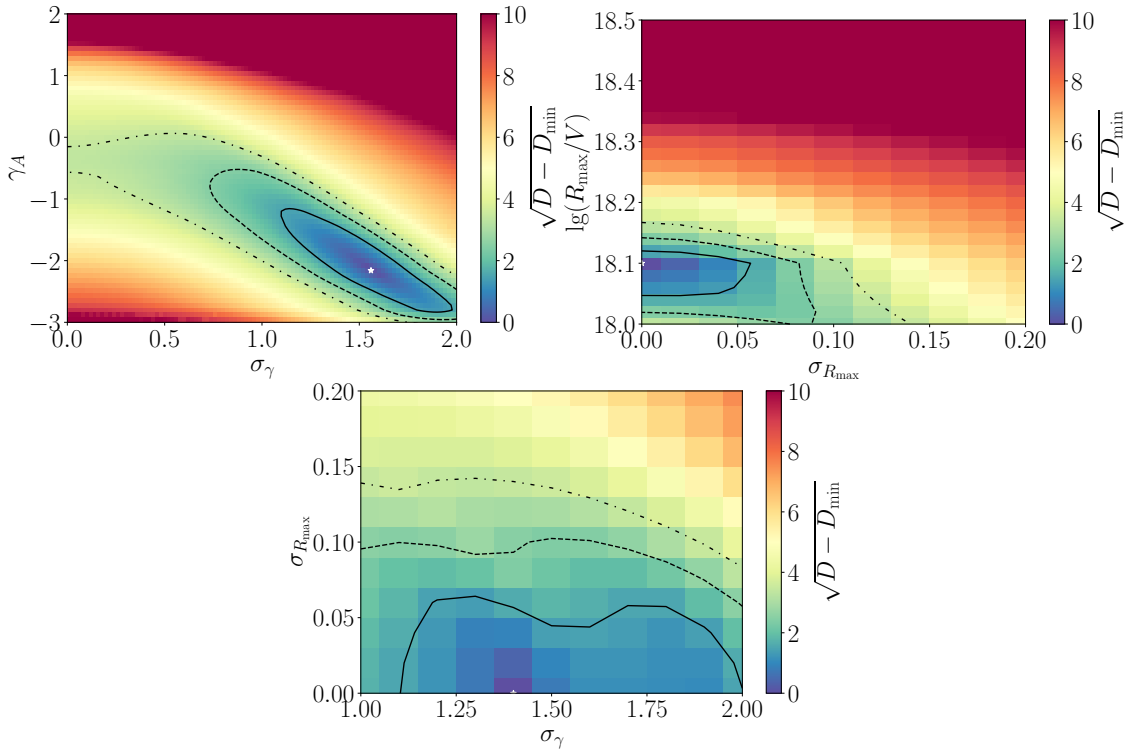

Figure 3: *Top-left*: Evolution of the deviance of the fit scanning the parameters the space σ_γ-γ for $\sigma_{R_{\max}} = 0$. *Top-right*: Evolution of the deviance of the fit scanning the parameters the space $\sigma_{R_{\max}}$-lg $R_{\max}$ for $\sigma_\gamma = 1.4$. *Bottom*: Evolution of the deviance of the fit scanning the parameters the space σ_γ-$\sigma_{R_{\max}}$. The solid, dashed and dot-dashed lines indicate the one, two and three sigma confidence intervals for two degrees of freedom. The white star indicates the position of the best minimum in each case.

References

[1] A. Aab et al., *NIM A* **798** (2015) 172, [1502.01323].
[2] A. Aab et al., *Science* **357** (2017) 1266-1270, [1709.07321].
[3] A. Aab et al., *Phys. Rev. D* **102** 062005 (2020), [2008.06486].
[4] AA. Halim et al., PoS(ICRC2023)**319**.
[5] AA. Halim et al., *JCAP* **05** (2023) 024, [2211.02857].
[6] D. Biehl et al., *A&A* **611** (2018) A101, [1705.08909].
[7] Q. Luce et al., *ApJ* **936** (2022) 62, [1409.5083].
[8] S. Marafico et al., *ApJ* **972** (2024) 4, [2405.17179].
[9] J. Biteau, *ApJS* **256** (2021) 15, [2105.11345].
[10] D. Ehlert et al., *Phys. Rev. D* **107** 103045 (2023), [2207.10691].
[11] Q. Yuan et al., *Phys. Rev. D* **84** 043002 (2011), [1109.0076].
[12] D. Ehlert et al., *JCAP* **02** (2023) 022, [2304.07321].
[13] P. Abreu et al., Eur. Phys. J. C **81** 966 (2021), [2109.13400].
[14] A. Aab et al., *Phys. Rev. D* **90** 122005 (2014), [1409.4809].
[15] A. Aab et al., *Phys. Rev. D* **90** 122006 (2014), [1409.5083].
[16] AA. Halim et al., *JCAP* **01** (2024) 022, [2305.16693].